# Spin-Orbit-Induced Topological Flat Bands in Line and Split Graphs of Bipartite Lattices

Da-Shuai Ma,[1,2] Yuanfeng Xu,[3] Christie S. Chiu,[4,5] Nicolas Regnault,[6,1]
Andrew A. Houck,[4] Zhida Song,[1] and B. Andrei Bernevig[1,*]

[1]*Department of Physics, Princeton University, Princeton, New Jersey 08540, USA*
[2]*Beijing Key Laboratory of Nanophotonics and Ultrafine Optoelectronic Systems, School of Physics, Beijing Institute of Technology, Beijing 100081, China*
[3]*Max Planck Institute of Microstructure Physics, 06120 Halle, Germany*
[4]*Department of Electrical Engineering, Princeton University, Princeton, New Jersey 08540, USA*
[5]*Princeton Center for Complex Materials, Princeton University, Princeton, New Jersey 08540, USA*
[6]*Laboratoire de Physique de l'École normale supérieure, ENS, Université PSL, CNRS, Sorbonne Université, Université Paris-Diderot, Sorbonne Paris Cité, Paris 75005, France*

(Received 22 August 2020; accepted 2 December 2020; published 31 December 2020)

Topological flat bands, such as the band in twisted bilayer graphene, are becoming a promising platform to study topics such as correlation physics, superconductivity, and transport. In this Letter, we introduce a generic approach to construct two-dimensional (2D) topological quasiflat bands from line graphs and split graphs of bipartite lattices. A line graph or split graph of a bipartite lattice exhibits a set of flat bands and a set of dispersive bands. The flat band connects to the dispersive bands through a degenerate state at some momentum. We find that, with spin-orbit coupling (SOC), the flat band becomes quasiflat and gapped from the dispersive bands. By studying a series of specific line graphs and split graphs of bipartite lattices, we find that (i) if the flat band (without SOC) has inversion or $C_2$ symmetry and is nondegenerate, then the resulting quasiflat band must be topologically nontrivial, and (ii) if the flat band (without SOC) is degenerate, then there exists a SOC potential such that the resulting quasiflat band is topologically nontrivial. This generic mechanism serves as a paradigm for finding topological quasiflat bands in 2D crystalline materials and metamaterials.

DOI: 10.1103/PhysRevLett.125.266403

*Introduction.*—New developments in the field of many-body condensed matter physics, such as twisted bilayer graphene (TBLG) [1–8], have underlined the importance of flat bands in realizing superconductivity and magnetism. In TBLG, a series of almost flat bands show a remarkable series of superconducting and magnetic states [5,6,8–28]. It is, however, known [29] that flat bands in Ginzburg-Landau theory result in a vanishing superfluid weight and hence no superconductivity. This is due to the fact that most flat bands are localized, the flatness usually resulting from atomiclike orbitals. It was recently argued that topology can save a flat band's superfluid weight: Chern bands support a lower bound on the superfluid density [30], while a more exotic type of topology, present in TBLG [31–33] that exhibits zero Chern number, can also place a lower bound on the superfluid weight [34–36]. Heuristically, topological bands contain extended states, which participate in the superconductivity [37–45]. As such, it is important to build flat bands with topological properties.

In this Letter, we present one generic method of building topological flat bands in crystals with spin-orbit coupling (SOC). A large number of these so-obtained topological flat bands are strong topological and exhibit the quantum spin Hall (QSH) effect, and the others are spinful fragile topological bands. Fragile topological flat bands also have been found in SOC-free systems [46], based on line graphs of nonbipartite lattices. It is well known that both line and split graph lattices exhibit flat bands in their spectra [47–53]. These bands are generally thought to be spanned by localized states [47] or contain a delocalized state due to a metallic band touch [54]. However, we find that, if certain symmetries are maintained, the states in the flat band cannot be localized and are topological. By adding spin-orbit coupling to line and split graphs of bipartite lattices, we gap the previously flat but gapless exact flat band into an quasiflat band that is topological. This provides us with a generic way to obtain flat bands with nontrivial topology.

*Nontrivial flat bands in the kagome lattice.*—A graph $(X)$ is bipartite if all of the vertices in the graph can be divided into two sets, $U$ and $V$, such that the edges in $X$ always connect a vertex in $U$ to a vertex in $V$. The honeycomb lattice is a well-known bipartite lattice with the two sets of vertices being the two sublattices. A line graph $L(X)$ of a graph $X$, which we will refer to as the root graph, is constructed by replacing each edge $e_{X,i}$ in $X$ with a vertex $v_{L(X),i}$ and connecting vertex pairs $v_{L(X),i}$ and $v_{L(X),j}$ for adjacent $e_{X,i}$ and $e_{X,j}$. As schematically shown in Fig. 1(a), the line graph of the honeycomb lattice is the kagome

 

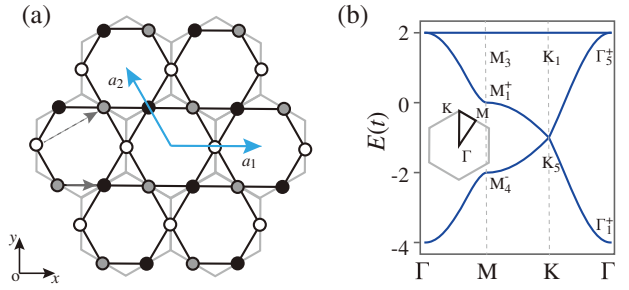


FIG. 1. (a) Schematic of the kagome lattice (black). One can obtain the lattice by applying the line graph operation on the honeycomb lattice (light gray). The light blue arrows indicate the lattice vectors $\boldsymbol{a}_1$ and $\boldsymbol{a}_2$. The white, black, and gray dots represent sites in the $A$, $B$, and $C$ sublattices, respectively. Nearest-neighbor (next-nearest-neighbor) SOC is introduced via hopping along the gray (dashed gray) arrow direction with amplitude $i\lambda_{NN}$ ($i\lambda_{\mathrm{NNN}}$). (b) The band structure for the kagome lattice without SOC. The irreducible representations (irreps) of each band at the high-symmetry points are shown. The superscript $+/-$ denotes the parity.

lattice. A split graph $S(X)$ is constructed from a root graph $X$ by placing an additional vertex on each edge $e_{X,i}$, as exemplified in Figs. 3(a) and 3(b).

Additional details about the bipartite lattice, line graph, and split graph are discussed in the Supplemental Material [55]. Here we only list some basic properties of these graphs [57,58]. We only consider 2D root graphs $X$ whose edges do not cross each other. For a bipartite lattice $X$ with $m$ polygon faces per unit cell, we have the following properties: (i) $X$ is a bipartite lattice if and only if all the polygons in $X$ are even sided. (ii) The band structure of $L(X)$ consists of a set of dispersive bands plus an additional set of flat bands at $E=-2t$, where $t$ is the hopping strength between two adjacent vertices and will be set as $-1$ in this Letter. The degeneracy of the flat bands of $L(X)$ is $D=m$. (iii) Its split graph $S(X)$ is always bipartite. (iv) There is a set of flat bands with degeneracy $D=m$ at $E=0$ in the energy spectrum of both $S(X)$ and $L[S(X)]$. (v) The flat bands of both $L(X)$, $S(X)$, and $L[S(X)]$ always touch the dispersive bands through a more highly degenerate state at some high-symmetry momenta.

The kagome lattice is the line graph of the honeycomb lattice, which is a bipartite lattice, as depicted in Fig. 1(a). There are three sublattices $A$, $B$ and $C$ in the kagome lattice. The three atoms of these sublattices are located at $(\frac{1}{2},0)$, $(0,\frac{1}{2})$, and $(\frac{1}{2},\frac{1}{2})$ within each unit cell, respectively. Here the coordinates are in units of the lattice vectors $\boldsymbol{a}_1=a(1,0)$ and $\boldsymbol{a}_2=a(-1,\sqrt{3})/2$ with $a$ being the lattice parameter.

The tight-binding model of the spinless lattice reads

$$H_0=t\sum_{\langle i,j\rangle}(c_i^\dagger c_j+\mathrm{H.c.}), \tag{1}$$

where $t=-1$ is the nearest-neighbor hopping, $\langle i,j\rangle$ denotes nearest-neighbor pairs, and $c_i^\dagger$ is the creation operator of an electron on lattice site $i$. One can diagonalize the model in momentum space, and the explicit form of the model Hamiltonian is then

$$H_0(\boldsymbol{k})=-2\begin{pmatrix}0&\cos\boldsymbol{k}_3&\cos\boldsymbol{k}_2\\ \cos\boldsymbol{k}_3&0&\cos\boldsymbol{k}_1\\ \cos\boldsymbol{k}_2&\cos\boldsymbol{k}_1&0\end{pmatrix}, \tag{2}$$

with $\boldsymbol{k}_i=\boldsymbol{k}\cdot\boldsymbol{a}_i/2$ and $\boldsymbol{a}_3=-\boldsymbol{a}_1-\boldsymbol{a}_2$.

The band structure of the kagome lattice is shown in Fig. 1(b). The band structure consists of a single flat band and two dispersive bands. The flat band touches one of the dispersive bands at the Γ point.

The development of topological quantum chemistry (TQC) [59–63] enables an efficient way to diagnose the topological phases from the symmetry-data vector (defined in the Supplemental Material [55]) of Bloch states at high-symmetry momenta. From TQC, the symmetry-data vector of any set of bands that cannot be decomposed into a linear combination of elementary band representations (EBRs), which are topologically equivalent with atomic orbitals in terms of the symmetry-data vector, is topological [59]. In the present Letter, we analyze the topological properties of the models in the language of TQC.

The model in Eq. (2) consists of spinless $s$ orbitals centered at the Wyckoff position $3f$ of the space group $P6/mmm$ (space group No. 191). The band representation (BR) of the full set of bands in Fig. 1(b) is $\{\Gamma_1^+\oplus\Gamma_5^+, \mathrm{K}_1\oplus\mathrm{K}_5, \mathrm{M}_1^+\oplus\mathrm{M}_3^-\oplus\mathrm{M}_4^-\}$. The character table of each irreducible representation (irrep) forming this BR is given in the Supplemental Material [55]. From TQC, this BR is a single EBR $(A_g)_{3f}\uparrow G$, which is induced from the $A_g$ orbital at the Wyckoff position $3f$ of the space group $P6/mmm$. As shown in Fig. 1(b), the irrep of the flat band at the M point is $\mathrm{M}_3^-$ with parity of $-1$. There is additionally a band touching between the flat band and a dispersive band at Γ with a two-dimensional (2D) irrep $\Gamma_5^+$, of which the parity is $+2$. In the presence of SOC, the 2D spinless irrep $\Gamma_5^+$ splits into two 2D spinful irreps with parity of $+2$. For spinful systems with inversion symmetry, the $\mathbb{Z}_2$ topological index $\nu$ is defined as $(-1)^\nu=\prod_{2n,j}P_{2n,j}$, where $P_{2n,j}$ is the parity of the $2n$th valence band at the $j$th time-reversal invariant momentum (TRIM) [64]. As any perturbative SOC does not change the parities of the bands at both Γ and M points, once the band touching at the Γ point is gapped by the symmetry-preserving SOC, one will always obtain one topologically nontrivial quasiflat band with $\nu=1$, resulting in a QSH insulator.

To identify the topology of the kagome lattice with SOC, we expand the basis of the model in Eq. (2) to $\{A,B,C\}\otimes\{\uparrow,\downarrow\}$ to include the spin degree of freedom. As schematically shown in Fig. 1(a), we take both the

nearest-neighbor (NN) and the next-nearest-neighbor (NNN) SOC with respective amplitudes $i\lambda_{\mathrm{NN}}$ and $i\lambda_{\mathrm{NNN}}$ into account. Then, the spinful model of the kagome lattice reads [65]

$$H(\boldsymbol{k}) = H_0(\boldsymbol{k}) \otimes \sigma_0 + [H_{\mathrm{NN}}(\boldsymbol{k}) + H_{\mathrm{NNN}}(\boldsymbol{k})] \otimes \sigma_z, \quad (3)$$

with

$$H_{\mathrm{NN}}(\boldsymbol{k}) = i2\lambda_{\mathrm{NN}} \begin{pmatrix} 0 & -\cos\boldsymbol{k}_3 & \cos\boldsymbol{k}_2 \\ -\cos\boldsymbol{k}_3 & 0 & -\cos\boldsymbol{k}_1 \\ \cos\boldsymbol{k}_2 & -\cos\boldsymbol{k}_1 & 0 \end{pmatrix} \quad (4)$$

and

$$H_{\mathrm{NNN}}(\boldsymbol{k}) = i2\lambda_{\mathrm{NNN}} \begin{pmatrix} 0 & -\cos\boldsymbol{k}'_1 & \cos\boldsymbol{k}'_2 \\ -\cos\boldsymbol{k}'_1 & 0 & -\cos\boldsymbol{k}'_3 \\ \cos\boldsymbol{k}'_2 & -\cos\boldsymbol{k}'_3 & 0 \end{pmatrix}, \quad (5)$$

where $\boldsymbol{k}'_i = \boldsymbol{k}_j - \boldsymbol{k}_k (i \neq j \neq k)$.

In the presence of NN or NNN SOC, the band touch at the Γ point will be removed, as shown in Figs. 2(a) and 2(b). Although the upper flat band becomes weakly dispersive, we can regard it as quasiflat when the amplitude of SOC is much smaller than $t$, as seen in Figs. 2(a) and 2(b), which is the case experimentally [66].

With SOC, the BR of the entire set of bands of kagome lattice is $\{\bar{\Gamma}_7 \oplus \bar{\Gamma}_8 \oplus \bar{\Gamma}_9, \bar{\mathrm{M}}_5 \oplus 2\bar{\mathrm{M}}_6, \bar{\mathrm{K}}_7 \oplus \bar{\mathrm{K}}_8 \oplus \bar{\mathrm{K}}_9\}$, which is an EBR $(\bar{E}_g)_{3f}\uparrow G$ induced from the $\bar{E}_g$ orbital at the Wyckoff position $3f$ of the double space group $P6/mmm$. Originating from the irrep pairs $\bar{\Gamma}_7$ and $\bar{\Gamma}_8$ switching partners in energy, the symmetry-data vector of the quasiflat band must be $\{\bar{\Gamma}_7, \bar{\mathrm{M}}_6, \bar{\mathrm{K}}_9\}$ or $\{\bar{\Gamma}_8, \bar{\mathrm{M}}_6, \bar{\mathrm{K}}_9\}$. One can get $\{\bar{\Gamma}_7, \bar{\mathrm{M}}_6, \bar{\mathrm{K}}_9\}$ ($\{\bar{\Gamma}_8, \bar{\mathrm{M}}_6, \bar{\mathrm{K}}_9\}$) by introducing NN (NNN) SOC, as shown in Figs. 2(a) and 2(b), respectively. Within the TQC theory, it is well known that, if some sets of bands separated by a band gap, and the symmetry-data vector of these sets of bands can be summed to a single EBR, then each set of bands possesses nontrivial topology. In both NN and NNN SOC added cases, the symmetry-data vector of the flat bands is not a linear combination of EBRs where all coefficients are positive integers. Thus, the quasiflat band is inevitably topologically nontrivial when either NN or NNN SOC is added. To verify the topology, one can obtain $\nu = 1$ from the parities of four TRIM points: $+1$ at the Γ point and $-1$ at three M points.

Apart from the symmetry-data vector and the $\mathbb{Z}_2$ index $\nu$, nontrivial topology of the flat bands can also be diagnosed from the Wilson loop method and the edge-state calculation. As shown in Fig. 2(c), an odd winding number of the Wilson loop can be found, indicating $\nu = 1$. By setting the strength of NN SOC as $\lambda_{\mathrm{NN}} = 0.1t$, we also perform the edge-state calculation of the kagome lattice with a finite size along the $x$ direction. As shown in Fig. 2(d), the presence of a gapless edge state between the flat band and dispersive band reflects the nontrivial topology of the flat band. In fact, for the lower dispersive band, we also have $\nu = 1$. Hence, there is another gapless state between the two dispersive bands.

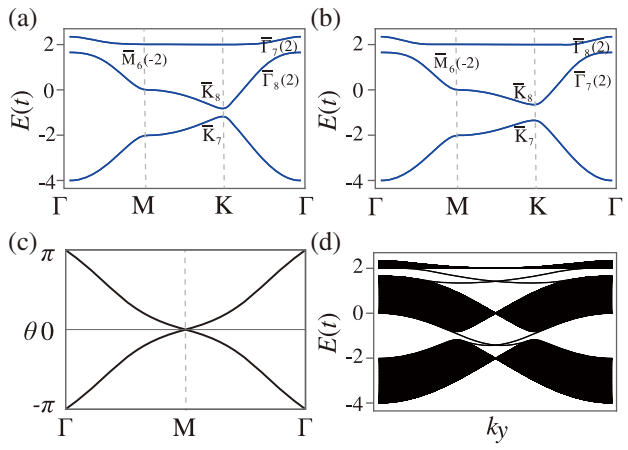


FIG. 2. (a),(b) Energy spectrum of the kagome lattice with (a) $\lambda_{\mathrm{NN}} = 0.1t$, $\lambda_{\mathrm{NNN}} = 0$; (b) $\lambda_{\mathrm{NNN}} = -0.1t$, $\lambda_{\mathrm{NN}} = 0$. The irreps are given, with numbers in brackets indicating the character of inversion symmetry. (c) The Wilson loop of the upper flat band with parameters $\lambda_{\mathrm{NN}} = 0.1t$, $\lambda_{\mathrm{NNN}} = 0$. (d) The band structure of the kagome lattice with finite size along the $x$ direction.

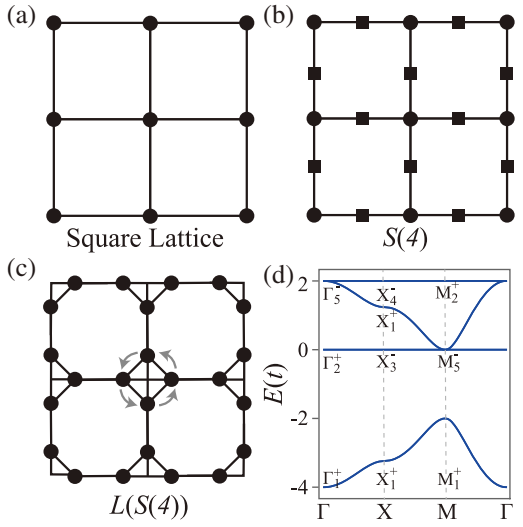


FIG. 3. (a) Schematic of the square lattice. (b) The split graph of square lattice $S(4)$. This lattice is also known as Lieb lattice. Placing a vertex (black square) at the middle of each edge in square lattice, and considering these vertices together with the vertices and edges of square lattice, we form the split graph $S(4)$. (c) The line graph of $S(4)$. The arrows in gray indicate that the amplitude of the considered SOC is $i\lambda$ when the spin-up electrons hop in this direction. (d) The structure of $S(4)$ without SOC. The irreps of each band at the high-symmetry points are shown. The superscript $+/-$ denotes the parity.

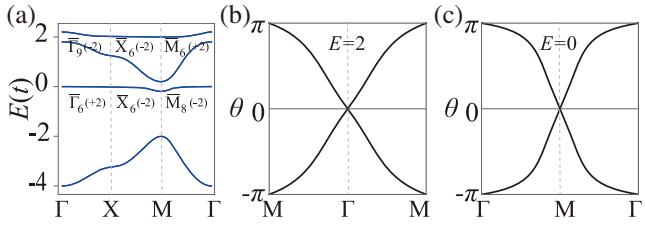


FIG. 4. (a) The band structure of the line graph of $S(4)$ with nearest-neighbor SOC of amplitude $0.1t$. There will be four separated sets of bands. The irreps are given, with numbers in brackets indicating the character of inversion symmetry. The Wilson loop of the quasiflat bands at (b) $E = 2$ and (c) $E = 0$.

*Nontrivial flat bands in the line graph of the $S(4)$ lattice.*—In this section, we introduce the flat bands in line graphs of another kind of bipartite lattice, i.e., the split graphs $S(X)$ of bipartite lattice $X$. As an example, the square lattice, its split graph $S(4)$, and the line graph of $S(4)$ are shown in Figs. 3(a)–3(c), respectively.

According to the basic properties, line graphs of $S(X)$ possess gapless flat bands at $E = 0$ and $E = 2$, as shown in Fig. 3(d). The BR of the full set of bands is a linear combination of several EBRs in space group $P4/mmm$, $(A_{1g})_{1a}\uparrow G + (B_{1g})_{1a}\uparrow G + (E_u)_{1a}\uparrow G$. The symmetry-data vector of the upper three bands is $\{\Gamma_5^- \oplus \Gamma_2^+, \mathrm{M}_5^- \oplus \mathrm{M}_2^+, \mathrm{X}_1^+ \oplus \mathrm{X}_3^- \oplus \mathrm{X}_4^-\}$, which is also a linear combination of EBRs $(B_{1g})_{1a}\uparrow G + (E_u)_{1a}\uparrow G$. Both $\mathrm{M}_5^-$ and $\Gamma_5^-$ are 2D irreps with parity $-2$. In contrast, both $\mathrm{M}_2^+$ and $\Gamma_2^+$ are 1D irreps with parity $+1$. As a result, as shown in Fig. 3(d), both of the flat bands at $E = 0$ and $E = 2$ have opposite parities at the M and Γ points. Thus, when the band touch is removed by introducing a symmetry-preserving SOC, the $\mathbb{Z}_2$ index becomes $\nu = 1$ for each of the flat bands, indicating a strong topological phase.

Upon adding NN SOC with strength $0.1t$, as shown in Fig. 4(a), both of the band touches at the Γ and M points are simultaneously gapped by the SOC. The Wilson loop calculations of the quasiflat bands at $E = 2$ and $E = 0$ are shown in Figs. 4(b) and 4(c), where the topologically nontrivial phase is indicated by an odd winding number of the Wilson loop.

*Discussion and conclusion.*—We find that, with SOC, the quasiflat bands in the kagome lattice and $L[S(4)]$ lattices are topologically nontrivial. In both cases, the degenerate point forms a 2D band representation with character of the inversion symmetry equal to 2 or $-2$. Since the space groups of these lattices are overgroups of $P2/m$, where no band degeneracy is enforced by symmetry, there is always one inversion-symmetry-maintained SOC that can remove the band touch and leave a set of gapped quasiflat bands. With nonzero $\mathbb{Z}_2$ index, these gapped quasiflat bands must be topologically nontrivial. We also explore the line graph of square lattice $L(4)$ and the line graph of the split lattice of the honeycomb lattice $L[S(6)]$; see Sec. III in the Supplemental Material for details [55]. Similar to that of the kagome and $L[S(4)]$ lattices, the band touches in the $L(4)$ and $L[S(6)]$ lattices form 2D irreps. Quasiflat bands result from adding SOC, and they are also topologically nontrivial with $\mathbb{Z}_2$ index $\nu = 1$. According to the basic properties (ii) and (iv), the degeneracy of the flat bands $D$ in $S(X)$ and $L(X)$ is well defined by the number of polygons per unit cell of bipartite root graph $X$. Apart from line graphs, which contain only one flat band (without SOC), one can design lattices with any fold degenerated flat bands as desired. The existence of degenerated flat bands is reported in photonic metacrystal [67]. Here, we provide a generic way to get degenerated flat bands in electronic materials. Such root graph lattices, including the octagon-square lattice and the hexagon-square lattice, which possess flat bands with $D = 2$, are studied in Sec. IV of the Supplemental Material [55]. With the nearest-neighbor SOC taken into consideration, we find the resulting set of quasiflat bands are also topologically nontrivial.

Split graphs of bipartite lattices comprise an entire class of lattices with flat bands. In contrast to the flat bands of the line graph lattices considered, the flat bands in these split graphs are at $E = 0$. We discuss the topological properties of these flat bands Sec. V of the Supplemental Material [55], where we find strong topological states. The finding of topological flat bands in split graph of bipartite lattice inspires us to extend our work to all bipartite lattices that keep $|n^U - n^V| > 0$ [55], where $n^U$ and $n^V$ are the numbers of vertices in $U$ and $V$, respectively. The flat band in dice lattice, a prominent example of such bipartite lattice, is discussed in detail in Sec. VI of the Supplemental Material [55], where the fragile topological state is found.

In summary, following the TQC theory, we investigate the topological properties of flat bands in line graphs and split graphs of bipartite lattices with symmetry-allowed SOC. For the line graph of $X$, there is a set of flat bands at $E = 2$, which becomes topologically nontrivial once the band touch is removed. For the line graph of $S(X)$, there are two sets of flat bands, one each at $E = 0$ and $E = 2$. Both of these sets of flat bands become topologically nontrivial when SOC is added. Finally, for split graphs of bipartite lattices, we find that adding Rashba SOC results in quasiflatbands that are strong topological. Since the symmetry-data vector of the quasiflat bands in our examples cannot be written purely as a sum of EBRs, at least one of the states in these quasiflat bands must be delocalized, in stark contrast to those of the flat bands in Ginzburg-Landau theory. Our results provide a generic way to obtain flat bands with nontrivial topology, as a path to explore strongly interacting systems.

B. A. B. thanks R. J. Cava, N. P. Ong, and A. Yazdani for discussions. This work was supported by the DOE Award No. DE-SC0016239, the Schmidt Fund for Innovative Research, Simons Investigator Grant No. 404513, and the Packard Foundation. Further support was provided

by the NSF-EAGER No. DMR 1643312, NSF-MRSEC No. DMR-1420541, ONR No. N00014-20-1-2303, Multidisciplinary University Research Initiative (MURI) W911NF-15-1-0397, Gordon and Betty Moore Foundation through Grant No. GBMF8685 toward the Princeton theory program, BSF Israel U.S. foundation No. 2018226, the Princeton Global Network Funds, China Postdoctoral Science Foundation Funded Project (Grant No. 2020M680011). Y. X. and B. A. also supported by Max Planck society.

*bernevig@princeton.edu

[1] J. M. B. Lopes dos Santos, N. M. R. Peres, and A. H. Castro Neto, Phys. Rev. Lett. **99**, 256802 (2007).
[2] E. Suárez Morell, J. D. Correa, P. Vargas, M. Pacheco, and Z. Barticevic, Phys. Rev. B **82**, 121407(R) (2010).
[3] R. Bistritzer and A. H. MacDonald, Proc. Natl. Acad. Sci. U.S.A. **108**, 12233 (2011).
[4] Y. Cao, V. Fatemi, A. Demir, S. Fang, S. L. Tomarken, J. Y. Luo, J. D. Sanchez-Yamagishi, K. Watanabe, T. Taniguchi, E. Kaxiras *et al.*, Nature (London) **556**, 80 (2018).
[5] Y. Cao, V. Fatemi, S. Fang, K. Watanabe, T. Taniguchi, E. Kaxiras, and P. Jarillo-Herrero, Nature (London) **556**, 43 (2018).
[6] X. Lu, P. Stepanov, W. Yang, M. Xie, M. A. Aamir, I. Das, C. Urgell, K. Watanabe, T. Taniguchi, G. Zhang *et al.*, Nature (London) **574**, 653 (2019).
[7] Y. Xie, B. Lian, B. Jäck, X. Liu, C.-L. Chiu, K. Watanabe, T. Taniguchi, B. A. Bernevig, and A. Yazdani, Nature (London) **572**, 101 (2019).
[8] A. L. Sharpe, E. J. Fox, A. W. Barnard, J. Finney, K. Watanabe, T. Taniguchi, M. Kastner, and D. Goldhaber-Gordon, Science **365**, 605 (2019).
[9] C. Xu and L. Balents, Phys. Rev. Lett. **121**, 087001 (2018).
[10] L. Zou, H. C. Po, A. Vishwanath, and T. Senthil, Phys. Rev. B **98**, 085435 (2018).
[11] M. Fidrysiak, M. Zegrodnik, and J. Spałek, Phys. Rev. B **98**, 085436 (2018).
[12] H. C. Po, L. Zou, A. Vishwanath, and T. Senthil, Phys. Rev. X **8**, 031089 (2018).
[13] H. Isobe, N. F. Q. Yuan, and L. Fu, Phys. Rev. X **8**, 041041 (2018).
[14] F. Wu, A. H. MacDonald, and I. Martin, Phys. Rev. Lett. **121**, 257001 (2018).
[15] E. Laksono, J. N. Leaw, A. Reaves, M. Singh, X. Wang, S. Adam, and X. Gu, Solid State Commun. **282**, 38 (2018).
[16] C.-C. Liu, L.-D. Zhang, W.-Q. Chen, and F. Yang, Phys. Rev. Lett. **121**, 217001 (2018).
[17] F. Wu, A. H. MacDonald, and I. Martin, Phys. Rev. Lett. **121**, 257001 (2018).
[18] Y. Su and S.-Z. Lin, Phys. Rev. B **98**, 195101 (2018).
[19] T. J. Peltonen, R. Ojajärvi, and T. T. Heikkilä, Phys. Rev. B **98**, 220504(R) (2018).
[20] D. M. Kennes, J. Lischner, and C. Karrasch, Phys. Rev. B **98**, 241407(R) (2018).
[21] F. Guinea and N. R. Walet, Proc. Natl. Acad. Sci. U.S.A. **115**, 13174 (2018).
[22] B. Roy and V. Juričić, Phys. Rev. B **99**, 121407(R) (2019).
[23] J. González and T. Stauber, Phys. Rev. Lett. **122**, 026801 (2019).
[24] B. Lian, Z. Wang, and B. A. Bernevig, Phys. Rev. Lett. **122**, 257002 (2019).
[25] K. Seo, V. N. Kotov, and B. Uchoa, Phys. Rev. Lett. **122**, 246402 (2019).
[26] M. Yankowitz, S. Chen, H. Polshyn, Y. Zhang, K. Watanabe, T. Taniguchi, D. Graf, A. F. Young, and C. R. Dean, Science **363**, 1059 (2019).
[27] T. Huang, L. Zhang, and T. Ma, Sci. Bull. **64**, 310 (2019).
[28] X.-C. Wu, K. A. Pawlak, C.-M. Jian, and C. Xu, arXiv: 1805.06906.
[29] D. Basov and A. V. Chubukov, Nat. Phys. **7**, 272 (2011).
[30] S. Peotta and P. Törmä, Nat. Commun. **6**, 8944 (2015).
[31] Z. Song, Z. Wang, W. Shi, G. Li, C. Fang, and B. A. Bernevig, Phys. Rev. Lett. **123**, 036401 (2019).
[32] J. Ahn, S. Park, and B.-J. Yang, Phys. Rev. X **9**, 021013 (2019).
[33] H. C. Po, L. Zou, T. Senthil, and A. Vishwanath, Phys. Rev. B **99**, 195455 (2019).
[34] F. Xie, Z. Song, B. Lian, and B. A. Bernevig, Phys. Rev. Lett. **124**, 167002 (2020).
[35] A. Julku, T. J. Peltonen, L. Liang, T. T. Heikkilä, and P. Törmä, Phys. Rev. B **101**, 060505(R) (2020).
[36] V. Peri, Z. Song, B. A. Bernevig, and S. D. Huber, arXiv: 2008.02288.
[37] S. Ryu, A. P. Schnyder, A. Furusaki, and A. W. Ludwig, New J. Phys. **12**, 065010 (2010).
[38] N. B. Kopnin, T. T. Heikkilä, and G. E. Volovik, Phys. Rev. B **83**, 220503(R) (2011).
[39] X.-L. Qi and S.-C. Zhang, Rev. Mod. Phys. **83**, 1057 (2011).
[40] B. A. Bernevig and T. L. Hughes, *Topological insulators and Topological Superconductors* (Princeton University Press, Princeton, NJ, 2013).
[41] M. Sato and Y. Ando, Rep. Prog. Phys. **80**, 076501 (2017).
[42] T. D. Stanescu, S. Tewari, J. D. Sau, and S. Das Sarma, Phys. Rev. Lett. **109**, 266402 (2012).
[43] G. Xu, B. Lian, P. Tang, X.-L. Qi, and S.-C. Zhang, Phys. Rev. Lett. **117**, 047001 (2016).
[44] M. Kheirkhah, Z. Yan, Y. Nagai, and F. Marsiglio, Phys. Rev. Lett. **125**, 017001 (2020).
[45] A. Lau, T. Hyart, C. Autieri, A. Chen, and D. I. Pikulin, arXiv:2008.09122.
[46] C. S. Chiu, D.-S. Ma, Z.-D. Song, B. A. Bernevig, and A. A. Houck, arXiv:2010.11953.
[47] A. Mielke, J. Phys. A **24**, L73 (1991).
[48] A. Mielke, J. Phys. A **24**, 3311 (1991).
[49] A. Mielke and H. Tasaki, Commun. Math. Phys. **158**, 341 (1993).
[50] J.-W. Rhim and B.-J. Yang, Phys. Rev. B **99**, 045107 (2019).
[51] F. C. de Lima, G. J. Ferreira, and R. Miwa, Phys. Chem. Chem. Phys. **21**, 22344 (2019).
[52] F. Crasto de Lima and G. J. Ferreira, Phys. Rev. B **101**, 041107(R) (2020).
[53] Z. Gao and Z. Lan, arXiv:2008.10738.
[54] D. L. Bergman, C. Wu, and L. Balents, Phys. Rev. B **78**, 125104 (2008).

[55] See Supplemental Material at http://link.aps.org/supplemental/10.1103/PhysRevLett.125.266403 for the proof of the properties of bipartite lattice, line and split graphs, character tables, and more examples where we find topological flat bands, which includes Ref. [56].
[56] E. H. Lieb, Phys. Rev. Lett. **62**, 1201 (1989).
[57] D. Cvetkovic, D. M. Cvetković, P. Rowlinson, S. Simic, and S. Simić, *Spectral Generalizations of Line Graphs: On Graphs with Least Eigenvalue-2* (Cambridge University Press, Cambridge, England, 2004), Vol. 314.
[58] A. J. Kollár, M. Fitzpatrick, P. Sarnak, and A. A. Houck, Commun. Math. Phys., **376**, 1909 (2020).
[59] B. Bradlyn, L. Elcoro, J. Cano, M. Vergniory, Z. Wang, C. Felser, M. Aroyo, and B. A. Bernevig, Nature (London) **547**, 298 (2017).
[60] L. Elcoro, B. Bradlyn, Z. Wang, M. G. Vergniory, J. Cano, C. Felser, B. A. Bernevig, D. Orobengoa, G. Flor, and M. I. Aroyo, J. Appl. Crystallogr. **50**, 1457 (2017).
[61] M. G. Vergniory, L. Elcoro, Z. Wang, J. Cano, C. Felser, M. I. Aroyo, B. A. Bernevig, and B. Bradlyn, Phys. Rev. E **96**, 023310 (2017).
[62] J. Cano, B. Bradlyn, Z. Wang, L. Elcoro, M. G. Vergniory, C. Felser, M. I. Aroyo, and B. A. Bernevig, Phys. Rev. B **97**, 035139 (2018).
[63] H. C. Po, H. Watanabe, and A. Vishwanath, Phys. Rev. Lett. **121**, 126402 (2018).
[64] L. Fu and C. L. Kane, Phys. Rev. B **76**, 045302 (2007).
[65] W. Beugeling, J. C. Everts, and C. Morais Smith, Phys. Rev. B **86**, 195129 (2012).
[66] J.-X. Yin, S. S. Zhang, G. Chang, Q. Wang, S. S. Tsirkin, Z. Guguchia, B. Lian, H. Zhou, K. Jiang, I. Belopolski *et al.*, Nat. Phys. **15**, 443 (2019).
[67] H. Wang, B. Yang, W. Xu, Y. Fan, Q. Guo, Z. Zhu, and C. T. Chan, Phys. Rev. A **100**, 043841 (2019).